Half-life of ^{51}Mn

Stephen A. Graves, Paul A. Ellison, Hector F. Valdovinos, Todd E. Barnhart, Robert J. Nickles, and Jonathan W. Engle

Phys. Rev. C **96**, 014613 — Published 18 July 2017

DOI: 10.1103/PhysRevC.96.014613

Half-life of ^{51}Mn

Stephen A. Graves, Paul A. Ellison, Hector F. Valdovinos,
Todd E. Barnhart, Jonathan W. Engle,* and Robert J. Nickles†
Department of Medical Physics,
University of Wisconsin-Madison,
Madison, WI 53705, USA

(Dated: May 22, 2017)

The half-life of ^{51}Mn was measured by serial gamma spectrometry of the 511 keV annihilation photon following decay by β^+ emission. Data were collected every 100 seconds for 100,000–230,000 seconds within each measurement (n = 4). The 511 keV incidence rate was calculated from the 511 keV spectral peak area and count duration, corrected for detector dead time and radioactive decay. Least-squares regression analysis was used to determine the half-life of ^{51}Mn while accounting for the presence of background contaminants, notably ^{55}Co. The result was 45.59 ± 0.07 min, which is the highest precision measurement to date and disagrees with the current Nuclear Data Sheets value by over 6σ.

I. INTRODUCTION

Positron-emitting isotopes of manganese have shown promise for a variety of medical applications in recent years [1–7]. Accurate and precise measurements of radioactive half-life are essential for quantitative biomedical studies.

During experimentation with ^{51}Mn, we observed that the half-life was shorter than the specified value of 46.2 ± 0.1 min from the most recent A=51 *Nuclear Data Sheets* evaluation [8]. Previous ^{51}Mn half-life measurements [9–14] are summarized in Table I. In light of the observed discrepancy from these values, we designed a dedicated experiment to measure the half-life of ^{51}Mn.

II. METHODS

^{51}Mn was produced by 16 MeV proton irradiation (GE PETtrace) of isotopically enriched ^{54}Fe (30–60 mg, 99.93% enriched, Isoflex USA), which had been electrodeposited over an area of $\sim$1 cm^2 on 0.5 mm thick, 21 mm diameter Ag discs. ^{51}Mn was radiochemically isolated from the target material by dissolution of the ^{54}Fe material followed by anion exchange chromatography as previously described [5]. An aliquot of ^{51}Mn (1–2 MBq in 20-100 μl) was then prepared for spectroscopic measurements.

A high-purity germanium (HPGe, Canberra C1519) gamma detector was calibrated for efficiency and energy response using point sources of ^{241}Am, ^{133}Ba, ^{137}Cs, and ^{60}Co obtained from the National Institute of Standards and Technology (NIST, Gaithersburg, MD, USA) and an in-house quantified point source of ^{152}Eu. Consecutive gamma spectra were for acquired with a ^{51}Mn sample in an unperturbed geometry for 25–60 hours. Acquisition lengths were set to 100 seconds live-time, resulting in 1000–2200 spectral time-points per measurement ($n = 4$). ^{51}Mn was produced prior to each measurement with a complete irradiation and radiochemical separation. Only one aliquot of ^{51}Mn from each production was used for a measurement. Due to the low branching ratio of the primary gamma emission of ^{51}Mn (749.07 keV, 0.265%), the 511 keV annihilation photon was utilized for half-life determination. Peak area was calculated by subtraction of an average background continuum determined from bins above and below the peak energy. Sensitivity of the measured half-life to changes in the count durations was evaluated by retrospectively re-binning spectral data into 500 second count durations.

Early spectral acquisitions were associated with up to 7% detector dead-time, resulting in $\sim$107 seconds elapsing (T_{real}) for a 100 second live-time (T_{live}) acquisition. In order to correct for radioactive decay during each acquisition, the initial 511 keV "incidence rate" (I_0) was obtained. If it is assumed that dead-time does not change significantly during a single acquisition, and that the nominal decay constant (λ) is sufficiently close to the true value, then the relationship between the number of counts in the 511 keV peak in a spectra (N) and I_0 is described by Equation 1.

$$N = \int_0^{T_{\text{real}}} \frac{T_{\text{live}}}{T_{\text{real}}} I_0 \mathrm{e}^{-\lambda t} dt \tag{1}$$

Evaluating this integral we obtain:

$$I_0 = \left(\frac{N}{T_{\text{live}}}\right)\left(\frac{\lambda T_{\text{real}}}{1 - \mathrm{e}^{-\lambda T_{\text{real}}}}\right) \tag{2}$$

It is also useful to make the following definition:

$$C \equiv \left(\frac{\lambda T_{\text{real}}}{1 - \mathrm{e}^{-\lambda T_{\text{real}}}}\right) \tag{3}$$

* jwengle@wisc.edu
† rnickles@wisc.edu

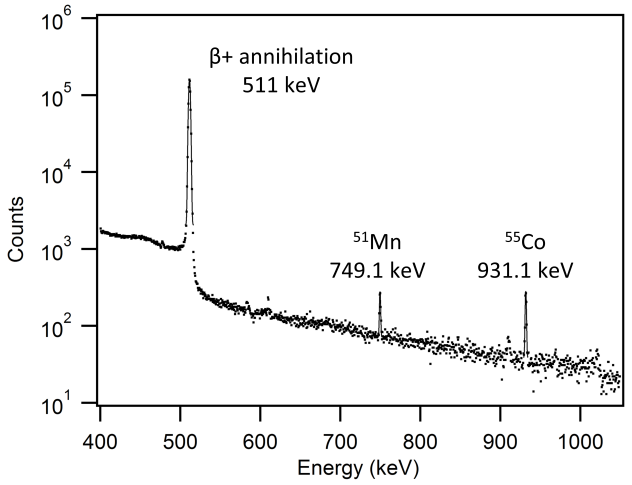

FIG. 1. Example HPGe gamma spectrum of ^{51}Mn with 3600 second count duration.

With this notation, C may be thought of as a correction factor for dead time and radioactive decay. For early time-points where dead-time was greater than 5%, this correction was 1.0133. For intermediate time-points where dead-time was less than 1% (511 keV peak area still ^{51}Mn-dominated), this corrective factor was reduced to 1.0126. At late time-points where ^{51}Mn had decayed below background levels, the decay constant for ^{55}Co was employed for this correction. During these late time-points, this correction was found to be less than 1.0006.

Radioactive contaminants were identified by summing the acquired spectra and identifying characteristic gamma emissions. Contaminants with direct contribution to the 511 keV peak included ^{55}Co, ^{56}Co, ^{208}Tl, and ^{106}Ag. Contaminants with indirect contribution to the 511 keV peak through pair production included ^{65}Zn, ^{214}Bi, ^{60}Co, ^{22}Na, ^{40}K, and ^{88}Y. Given that the half-lives of these contaminants are significantly greater than that of ^{51}Mn, the majority are well approximated by linear or constant background fitting components to the 511 keV incidence rate decay curve. ^{55}Co, likely produced from the (p,2n) reaction on ^{56}Fe impurities in the target material, was treated independently in decay fitting due to its shorter half-life and relatively high abundance.

Decay curve least-squares fitting was performed using the model described by Equation 2, where A_1, λ_1, A_2, λ_2, M, and C were fitting parameters. To specifically account for the presence of ^{55}Co, λ_2 was constrained to $\ln(2)/(63108\text{ s})$. Sensitivity of this constraint to the uncertainty in the nominal ^{55}Co half-life was evaluated. Fitting was performed over the full set of data for each run, without temporal truncation.

$$f(t) = A_1 e^{-\lambda_1 t} + A_2 e^{-\lambda_2 t} + Mt + C \qquad (4)$$

Initial least-squares fitting was weighted by the square-root of the measured 511 keV count-rate divided by the square root of the count duration. After this first-pass of curve fitting, fitting was performed weighted by a floating standard deviation of the first-pass fitting residuals. The width of this variance estimation window was nominally chosen to be 3000 seconds, centered at the sample of interest. It is not obvious that this window should be sample-centered, however application of the mean value theorem over 3000 seconds to an approximation of the uncertainty function (square root of count rate) reveals that this is appropriate. Fitting was performed iteratively using this weighting method until changes in obtained fitting parameters were negligible.

To ensure that data were not affected by drift in the digital acquisition clock, the CPU clock was compared against the web-based NIST clock. We observed a maximum drift of -7.6 ± 0.3 seconds in the CPU clock compared with the web-based NIST clock during a 68 hour acquisition. This deviation results in a correction to the measured ^{51}Mn half-life of less than 0.002 min, which is herein considered negligible.

All measurement and statistical uncertainty was assumed to be normally distributed for propagation calculations. All uncertainties in this work are presented as $\pm$ one standard deviation (σ).

III. RESULTS AND DISCUSSION

An example gamma spectrum is shown in Figure 1 and a representative decay curve and corresponding fit are shown in Figure 2. A final ^{51}Mn radioactive half-life value for ^{51}Mn of 45.59 ± 0.07 min was obtained. Results from individual measurements are listed in Table II, and the final result is compared against literature values in Table I.

TABLE I. Previous measurements of the radioactive half-life of ^{51}Mn, including the result from this work.

Reference	$t_{1/2} \pm \sigma$ (min)
Livingood, 1938 [9]	46 ± 2
Miller, 1948 [10]	45
Burgus, 1950 [11]	44.3 ± 0.5
Gilbert, 1966 [12]	46.5 ± 0.2
Erlandsson, 1969 [13]	46.2 ± 0.1
Ferrer, 1973 [14]	[46.2 ± 0.1][a]
This work	45.59 ± 0.07

[a] Authors state that their measurement is "in agreement with" Erlandsson et al..

This obtained half-life value does not agree with the most precise previous measurement, made by Erlandsson et al. in 1969 [13], of 46.2 ± 0.1 min, which is also the currently accepted value. In their work, Erlandsson et al. produced radioisotopically pure ^{51}Mn by ^{50}Cr(p,γ), and performed serial annihilation photon spectroscopic measurements — NaI(Tl) detector, 400–600 keV window — over approximately 6600 seconds. A single-component

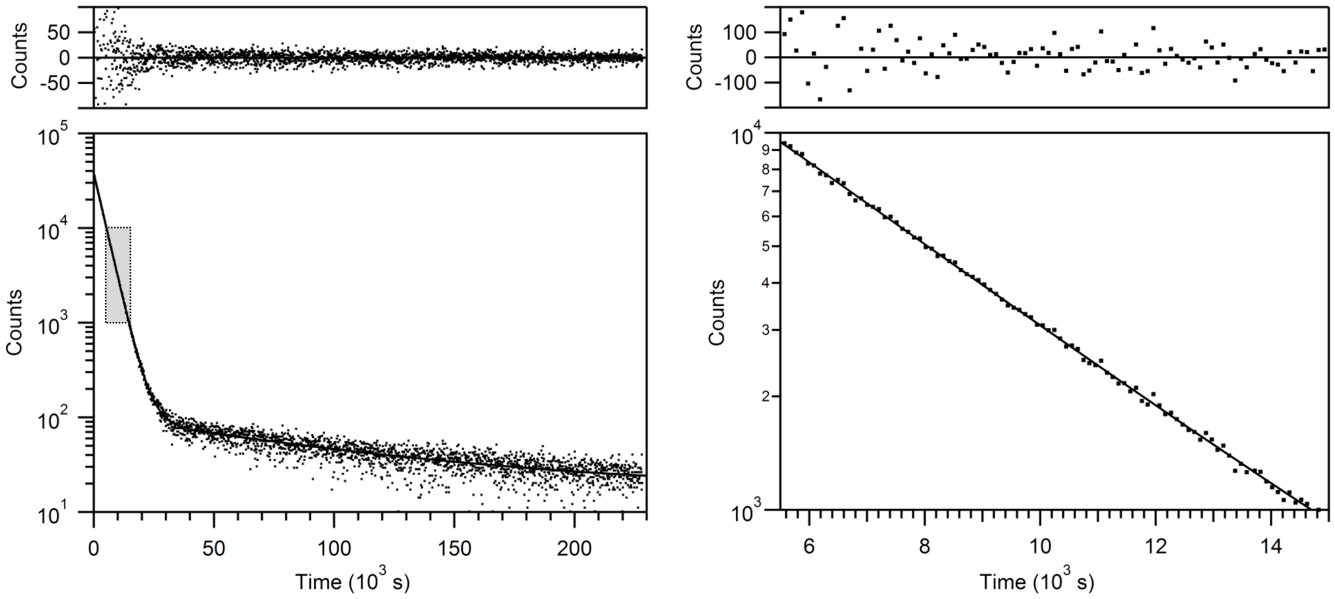

FIG. 2. Decay curve fitting for one representative measurement and associated fitting residuals. Serial spectroscopic measurements were acquired over approximately 230,000 seconds and the 511 keV peak fit by a two-component exponential and linear component decay curve. The right plot shows a subset of the full data set, over one decade of ^{51}Mn decay, indicated by the rectangle in the left plot.

TABLE II. ^{51}Mn half-life measurements in this work.

Measurement	$t_{1/2} \pm \sigma$ (s)	χ^2/dof
1	45.63 ± 0.06	1.004
2	45.56 ± 0.04	0.995
3	45.53 ± 0.04	1.001
4	45.66 ± 0.04	0.992
Average	45.59 ± 0.07	–

exponential model was used for decay fitting, which ignored contributions from background contaminants, such as the annihilation photons following pair production from the 1461 keV ^{40}K γ-emission.

Without considering other possible confounding factors, a plausible explanation for the shorter half-life result obtained herein is the presence of ^{52m}Mn in our radioactivity samples, however the 1434 keV characteristic ^{52m}Mn γ-emission was not observed.

In order to investigate this discrepancy, a truncated set of our data was created (0 – 20,000 s) and was fit to a single-component exponential model. The half-life result from this fitting (46.13 ± 0.04 min) is in excellent agreement with the literature value of 46.2 ± 0.1 min. However, if we fit this truncated data set to the full model described by Equation 2 constraining A_2, λ_2, M, and C to values obtained from fitting the full data set, a ^{51}Mn half-life value of 45.70 ± 0.04 min is obtained, which is in agreement with the value reported here. This constrained fit on data from t = 0 – 20,000 s also qualitatively improved the "goodness of fit" in the latter portion of the truncated data set compared with the unconstrained fit.

The robustness of radioisotopic impurity quantification in our regression model was examined. The most significant impurity, ^{55}Co, was quantified by fitting the decay of its characteristic 931 keV gamma over the collected serial spectra. ^{55}Co radioactivity at $t = 0$ was quantified by correcting for branching ratio and detector efficiency. This secondary quantification was in excellent agreement with the ^{55}Co radioactivity quantification obtained from the A_2 fitting parameter in 511 keV fitting, 12.8 ± 1.1 kBq and 12.3 ± 0.8 kBq respectively. This suggests that explicit fitting of ^{55}Co in the 511 keV regression model is appropriate and robust.

^{51}Mn half-life measurements did not depend strongly on the constrained half-life of ^{55}Co in decay curve fitting. Perturbing the constrained half-life of ^{55}Co (nominally 17.53 ± 0.03 h) for one measurement dataset by 10% to 15.77 h or 19.28 h results in a change to the measured ^{51}Mn half-life of less than 0.0002%. Furthermore, ^{51}Mn half-life measurements were not sensitive to changes in count duration. Retrospectively re-binning the acquired spectra into 500 second count durations resulted in no significant change to the measured half-life values.

An attempt was also made to quantify the half-life of ^{51}Mn using the 749.1 keV peak from the spectral data of one measurement. Data were re-binned into 1000 second acquisitions to improve statistics, and regression analysis was performed using a single exponential and background component; $f(t) = Ae^{-\lambda t} + C$. The result from this measurement was 50 ± 7 min, which suggests that a precise half-life evaluation using the 749.1 keV peak in our data is unfeasible.

The discrepancy between the measured half-life value

in this work (45.59 min) and the literature value (46.2 min) is a difference of approximately 1.3%. A difference of this degree could conceivably impact the results of preclinical biomedical studies through systematic error in decay correction. For example it is common to administer radioactivity to animal subjects several hours before tissue uptake is quantified. Assuming four hours of radioactive decay during this window, the discrepancy described herein results in a ∼5% systematic error in tissue uptake quantification. An error of this magnitude is not insignificant when compared with other sources of uncertainty in studies of this design. For this reason, we believe this work will serve to improve the accuracy of preclinical biomedical studies employing ^{51}Mn.

IV. CONCLUSION

The half-life of ^{51}Mn has been measured to be 45.59 ± 0.07 min. This is the most precise measurement to date, and disagrees with the Nuclear Data Sheets (NDS) value by over 6σ. Due to the improved fitting model and data acquisition duration in this work, we believe that this measurement is more accurate than previous literature values.

ACKNOWLEDGMENTS

This work was funded in part by the National Institutes of Health (T32-CA009206).

[1] G. J. Topping, P. Schaffer, C. Hoehr, T. J. Ruth, and V. Sossi, Med. Phys. **40** (2013).
[2] C. M. Lewis, S. A. Graves, R. Hernandez, H. F. Valdovinos, T. E. Barnhart, W. Cai, M. E. Meyerand, R. J. Nickles, and M. Suzuki, Theranostics **5**, 227 (2015).
[3] S. A. Graves, R. Hernandez, J. Fonslet, C. G. England, H. F. Valdovinos, P. A. Ellison, T. E. Barnhart, D. R. Elma, C. P. Theuer, W. Cai, R. J. Nickles, and G. W. Severin, Bioconjugate Chem. **26**, 2118 (2015).
[4] J. Fonslet, S. Tietze, A. I. Jensen, S. A. Graves, and G. W. Severin, Appl. Radiat. Isot. **121**, 38 (2017).
[5] S. A. Graves, R. Hernandez, H. F. Valdovinos, P. A. Ellison, J. W. Engle, T. E. Barnhart, and R. J. Nickles, "Preparation and in vivo characterization of $^{51}MnCl_2$ as PET tracer of Ca^{2+} channel-mediated transport," (2017), Sci. Rep.
[6] R. Hernandez, S. A. Graves, T. Gregg, C. G. England, H. F. Valdovinos, J. J. Jeffery, T. E. Barnhart, G. W. Severin, R. J. Nickles, M. J. Merrins, and W. Cai, "Radiomanganese PET detects changes in β-cell mass in mouse models of diabetes," Diabetes.
[7] A. L. Wooten, T. A. Aweda, B. C. Lewis, R. B. Gross, and S. E. Lapi, PloS one **12** (2017).
[8] H. Xiaolong, Nuclear Data Sheets **107**, 2131 (2006).
[9] J. J. Livingood and G. T. Seaborg, Phys. Rev. **54**, 391 (1938).
[10] D. R. Miller, R. C. Thompson, and B. B. Cunningham, Phys. Rev. **74**, 347 (1948).
[11] W. H. Burgus and J. W. Kennedy, Chem. Phys. **14** (1950).
[12] K. M. Gilbert and H. T. Easterday, Nuc. Phys. **86**, 279 (1966).
[13] B. Erlandsson, A. Marcinkowski, and N. Wall, Ark. Fys. **40**, 139 (1969).
[14] J. C. Ferrer and J. Rapaport, Z. Physik **265**, 365 (1973).